

Structure of *n*,3 Polyamides, a Group of Nylons with Two Spatial Hydrogen-Bond Orientations

J. Puiggali, J. E. Aceituno, E. Navarro, J. L. Campos, and J. A. Subirana*

Departament d'Enginyeria Química, ETS d'Enginyers Industrials, Universitat Politècnica de Catalunya, Diagonal 647, Barcelona 08028, Spain

Received January 16, 1996; Revised Manuscript Received July 3, 1996[®]

ABSTRACT: Models are presented for the family of *n*,3 polyamides. They have an organization in space quite different from the usual α and γ forms of polyamides. Hydrogen-bonded sheets are not present in the *n*,3 polyamides. The molecules are linked by an unique network of hydrogen bonds with two spatial orientations which form an angle of about 120°. The different organization of the molecules when *n* = odd (orthorhombic) and *n* = even (monoclinic) is shown to be due to the optimization of the hydrogen-bond geometry. The polymethylene segments deviate somewhat from an *all-trans* conformation.

Introduction

We have recently synthesized and characterized several *n*,3 polyamides.¹ The X-ray diffraction and electron microscopy results obtained, taken together with work carried out on low molecular weight model compounds studied by X-ray crystallography,^{2,3} indicate that these polymers are organized as a network of hydrogen-bonded molecules with two different hydrogen-bond orientations, with an angle of about 60° among them. Thus these nylons deviate significantly from the conventional structure of the common α form⁴ of nylon 66 and many other polyamides, which are organized as parallel sheets of hydrogen-bonded molecules. Its organization is also different from the structure suggested for the γ form,⁵ which is also organized in parallel sheets of hydrogen-bonded molecules.

The X-ray diffraction and electron microscopy results obtained with these *n*,3 polyamides have shown that the molecules crystallized in a different system depending on the value of *n*. When *n* is odd, an orthorhombic cell is found, whereas when *n* is even, a monoclinic cell appears. In order to understand this difference in behavior, we have synthesized and determined the structure of a low molecular weight model of nylon 5,3. With these results in hand and previous work^{1–3} already reported, we have been able to develop adequate three-dimensional models for the *n*,3 polyamides which we report in this paper.

Experimental Section

Synthesis of the Model Compound Nylon 5,3: *N*-Propyl-*N*'-[5-(((propylamino)malonyl)amino)pentyl]malonamide (pMPMp). pMPMp was prepared by a three-step synthesis outlined in Scheme 1. The monoethyl malonate and the *N*-propylmalonic acid ethyl ester were obtained according to previously reported methods^{3,6} and recrystallized prior to use. Other required reagents were obtained commercially and used without further purification.

***N*-Propyl-*N*'-[5-(((propylamino)malonyl)amino)pentyl]malonamide:** A 451 μ L (3.8 mmol) portion of 1,5-pentanediamine was added to 2.66 g (15.3 mmol) of *N*-propylmalonic acid ethyl ester (12 mmol). The reaction mixture was initially clear, but a white precipitate quickly developed. After 24 h, 20 mL of CHCl_3 was added and the slurry was filtered through a glass frit. The precipitate was recrystallized from water, giving a white powder in 63% yield. Mp: 217–219 °C. Chromatographic purity: 97%. Elution time: 5.35 min. IR

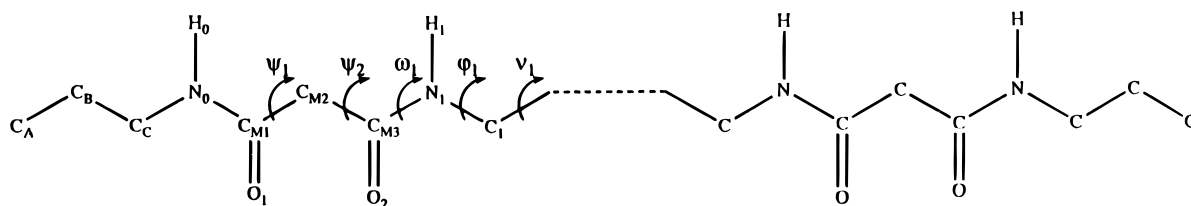
(ν , cm^{-1}): 3290 (amide A), 3095 (amide B), 2925 (C–H), 1632 (amide I), 1560 (amide II). ¹H-NMR (300 MHz, TFA-*d*): δ 3.51 (4H, s, CH_2 -mal), 3.18 (8H, 2t, $-\text{NHCH}_2\text{CH}_2\text{CH}_2-$ and $\text{CH}_2\text{CH}_2\text{CH}_3$), 1.41 (8H, 2t, $-\text{NHCH}_2\text{CH}_2\text{CH}_2-$ and $\text{CH}_2\text{CH}_2\text{CH}_3$), 1.21 (2H, m, $-\text{NHCH}_2\text{CH}_2\text{CH}_2-$), 0.72 (6H, t, $\text{CH}_2\text{CH}_2\text{CH}_3$). ¹³C-NMR (75.5 MHz, TFA-*d*): δ 173.83 ($-\text{CONH}(\text{CH}_2)_5-$), 172.83 ($\text{CH}_3\text{CH}_2\text{CH}_2\text{NHCO}$), 43.01 ($-\text{NHCH}_2\text{CH}_2\text{CH}_2-$), 45.44 ($\text{CH}_2\text{CH}_2\text{CH}_3$), 35.71 (CH_2 -malonyl), 29.45 ($-\text{NHCH}_2\text{CH}_2\text{CH}_2-$), 25.45 ($-\text{NHCH}_2\text{CH}_2\text{CH}_2-$), 23.07 ($\text{CH}_2\text{CH}_2\text{CH}_3$), 11.41 ($\text{CH}_2\text{CH}_2\text{CH}_3$). Anal. Calcd for $\text{C}_{17}\text{H}_{32}\text{N}_4\text{O}_4$: C, 57.28; N, 15.72; H, 9.05. Found: C, 57.17; N, 15.68; H, 9.06.

Characterization. Infrared (IR) spectra were obtained from KBr pellets using a Perkin-Elmer 783 spectrophotometer in the 4000–500 cm^{-1} range. Proton and carbon magnetic resonance (¹H and ¹³C NMR) spectra were obtained in deuterated trifluoroacetic acid using a Bruker AMX-300 spectrometer. Chemical shifts are reported in parts per million (δ) downfield from internal tetramethylsilane (TMS). Chromatographic purity was determined with an HPLC Shimadzu SCL-6B analyzer, using an RP-18 Spherisorb ODS-2 column (25 \times 0.4 cm; particle size 5 μ m). The column was eluted with 50% methanol in water and the flow rate was kept at 1 mL/min (λ = 220 nm).

X-ray Diffraction of the Model Compound pMPMp. Colorless lamellar crystals (1.1 \times 1.1 \times 0.1 mm³) were obtained by vapor diffusion (20 °C) from a water solution (concentration 2.88 mg/mL) against 50% (vol) aqueous 2-propanol used as precipitant. X-ray data were collected at room temperature using an Enraf-Nonius CAD-4 diffractometer with Cu K α radiation (λ = 1.54178 Å) and a graphite monochromator (2 θ < 136°, ω scanning mode). Three reflections were monitored every hour during data collection and showed little variation of intensity, indicating that the crystals were very stable to the X-rays. Intensity data were corrected for Lorentz and polarization effects, and absorption was disregarded. High values of *R*(int) and *R*(σ) were attained (13.65 and 7%, respectively) due to the fact that the crystals were very thin (about 0.1 mm) and had a great mosaicity, as deduced from the vertical line (ω scan direction) that appears on the ω – θ plot. Although two different unit cells (monoclinic and orthorhombic) were compatible with the collected data, we chose the monoclinic one, since we have not found any symmetry indicative of an orthorhombic space group. Moreover, the diffractogram did not fit with any Laue class belonging to an orthorhombic system. The resulting cell dimensions together with other experimental measures are given in Table 1. The structure was solved by direct methods using the SHELXS-86⁷ program and assuming a *P*12₁/*m*1 monoclinic symmetry. The *E*-map was calculated and revealed all the non-hydrogen atoms. The molecular structure was then refined by a full matrix least-squares procedure, SHELXS-93,⁸ with weights redetermined after each program run. Hydrogen atoms were included in stereochemically ideal positions. Anisotropic refinement for all non-hydrogen atoms and isotropic refine-

[®] Abstract published in *Advance ACS Abstracts*, November 1, 1996.

a)



b)

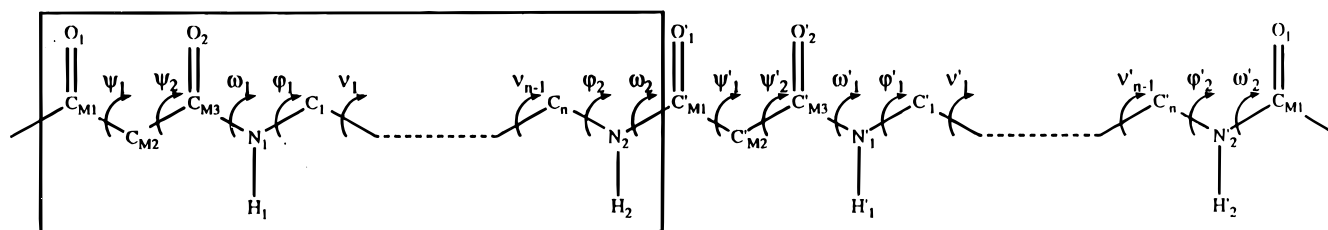
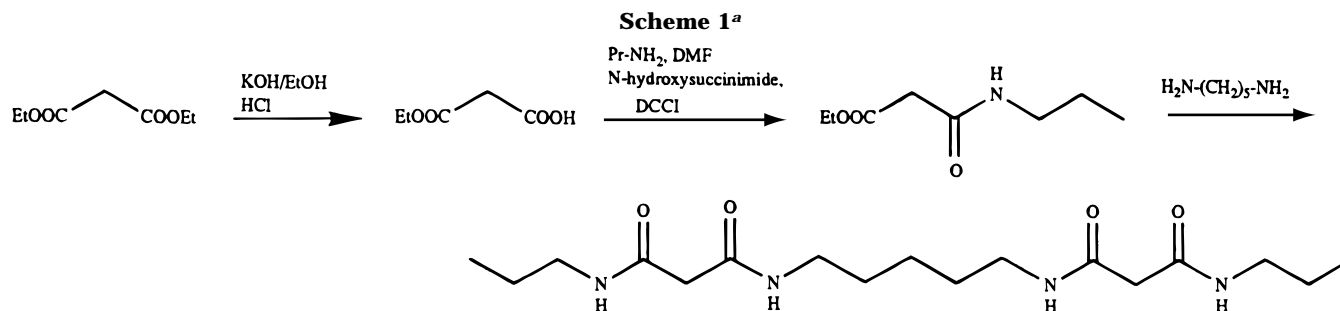


Figure 1. Atomic numbering scheme and torsional angles for the asymmetric unit of the model compounds discussed in this work (a) and for a generic nylon *n*,3 backbone (b).



^a Abbreviations: Et, ethyl; Pr, propyl; DCC, *N,N*-dicyclohexylcarbodiimide; DMF, *N,N*-dimethylformamide.

ment for hydrogens gave a final agreement factor of $R = 15.5\%$ and a goodness of fit (GOF) parameter = 0.877 for 968 reflections with $I < 2\sigma(I)$, using only the reflections with a resolution higher than 1 Å. The maximum and minimum heights in the final difference Fourier synthesis were 0.59 and $-0.35 \text{ e } \text{\AA}^{-3}$, respectively. The atomic scattering factors were taken from the International Tables for X-ray Crystallography (1974), and a micro-Vax 2000 computer was used for all computations.

Structural Modeling of Nylons *n*,3. The linked-atom least-squares (LALS) method⁹ was used to build and refine suitable models for nylons 5,3 and 6,3. The description of a generic residue of nylon *n*,3 is given in Figure 1a. Standard bond distances and bond angles for malonyl residues and polyamides were adopted to build the repeating unit and kept constant throughout the whole modeling process. Thus the only parameters needed to define the chain conformation were the torsion angles ψ_1 and ψ_2 of the malonyl residues, plus the diamine torsion angles ϕ_1 , ν_1 , and ϕ_2 . The amide torsion angles ω_1 have been kept in the *trans* conformation for all the models studied. The azimuthal angle μ which defines the orientation of the molecular chain in the unit cell was also allowed to vary during refinement.

Models were first refined taking into account (a) the experimental chain repeat length, (b) the packing constraints due to the unit cell dimensions, and (c) the optimum hydrogen-bond geometry. A second refinement was carried out with the introduction of the diffraction data obtained by electron microscopy from single crystals. Appropriate atomic structure factors for electron diffraction were used. Scaling and temperature factors were refined at this stage. Electron diffraction intensities were measured with a Joyce Loebel MK III CS microdensitometer and were used without further corrections

Table 1. Crystallographic Data for $\text{CH}_3(\text{CH}_2)_2\text{-NHCOCH}_2\text{CONH}(\text{CH}_2)_5\text{NHCOCH}_2\text{CONH}(\text{CH}_2)_2\text{CH}_3$ (pMPMp)

compound	pMPMp
molecular formula	$\text{C}_{17}\text{H}_{32}\text{N}_4\text{O}_4$
crystal size (mm^3)	$1.1 \times 1.1 \times 0.1$
crystal system	monoclinic
space group	$P2_1/m$
cell	
a (Å)	4.662(2)
b (Å)	51.45(1)
c (Å)	4.888(2)
α (deg)	90.0
β (deg)	118.29(3)
γ (deg)	90.0
volume (\AA^3)	1033(2)
Z (molecules/unit cell)	2
asymmetric unit (molecule)	1/2
calculated density (g/cm^3)	1.146
scanning mode	ω scan
collected reflections	3919 ($2\theta < 136^\circ$)
unique reflections	1814
$R(\text{int})^a$	0.1365
$R(\sigma)^a$	0.0700
observed reflections	968 (resolution 1 Å)
no. of refined parameters	117
goodness-of-fit on F^2	0.877
R factor	0.155
wR^2	0.429
min/max heights ($\text{e}/\text{\AA}^3$) in the difference Fourier map	$-0.35/0.59$

^a $R(\text{int}) = \sum |F^2 - (F)_{\text{mean}}| / \sum F^2$. $R(\sigma) = \sum \sigma(F^2) / \sum F^2$. $1/w = \sigma^2(F_0^2) + (0.3023P)^2 + 6.23P$, where $P = [\max(F_0^2, 0) + 2F_c^2/3]$.

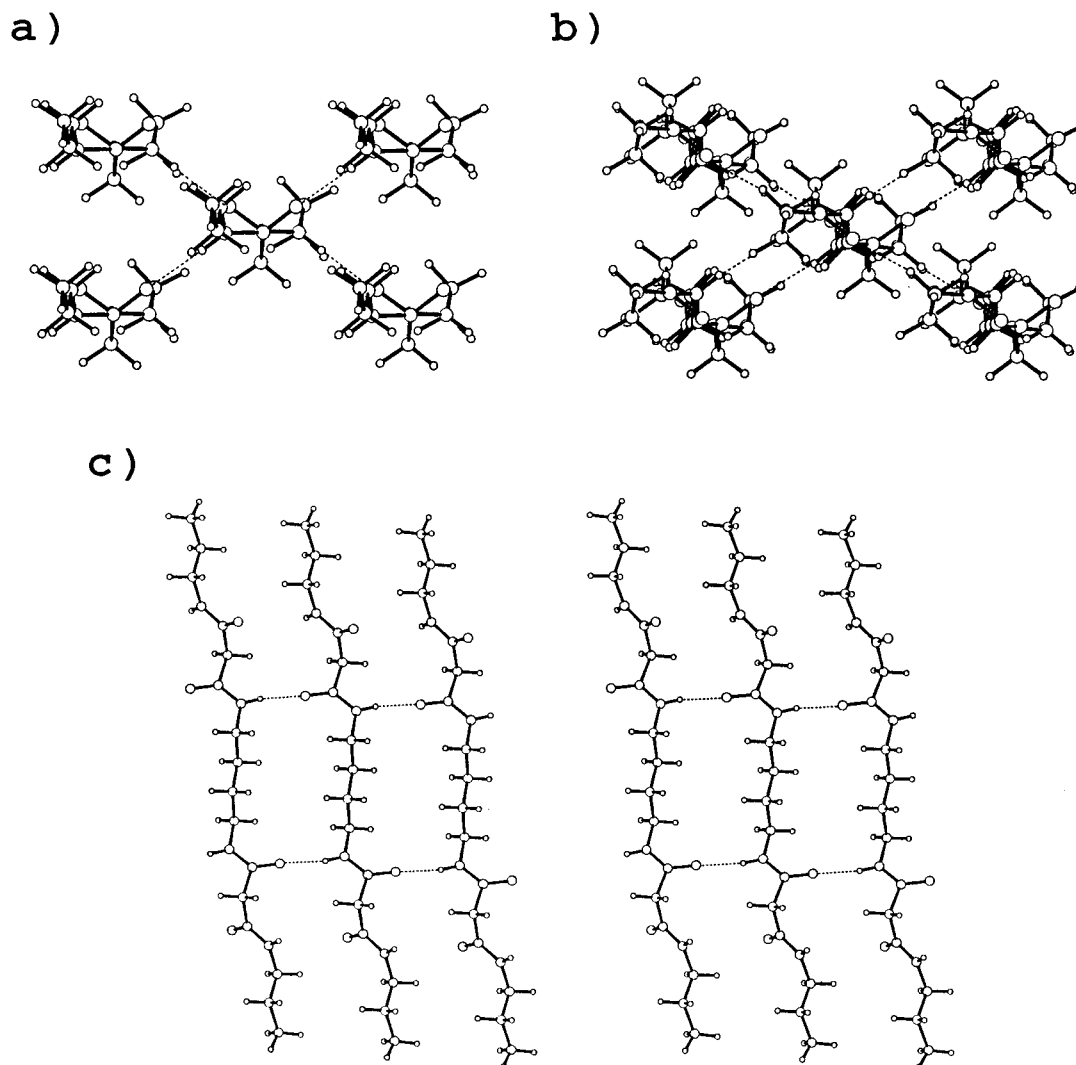


Figure 2. Projection of one layer of pMPMp (a) and pMBMp (b). A group of five molecules is shown. The hydrogen bonds of the central molecule with its four neighbors are indicated as dashed lines. (c) Stereopair showing the conformation in the crystalline state of three hydrogen-bonded molecules of pMBMp. Note that each malonyl residue produces a 120° rotation between amide planes.

as it is established for electron diffraction data. Due to the low lamellar thickness, dynamical scattering was neglected. Although fiber diffraction patterns of the two polymers were available,¹ the quality of the patterns was not sufficient to use quantitative intensity data for refinement purposes. Instead, fiber diffraction patterns of the models were simulated with the CERIUS 3.1 version (Molecular Simulations Inc.) to give a qualitative comparison. The peaks in the X-ray patterns were broadened with a Lorentzian profile in order to take into account the crystal size, and a disorientation angle was introduced in order to simulate the arched reflections. Calculations were run on a HP-340 computer and a Silicon Graphics Indigo Workstation.

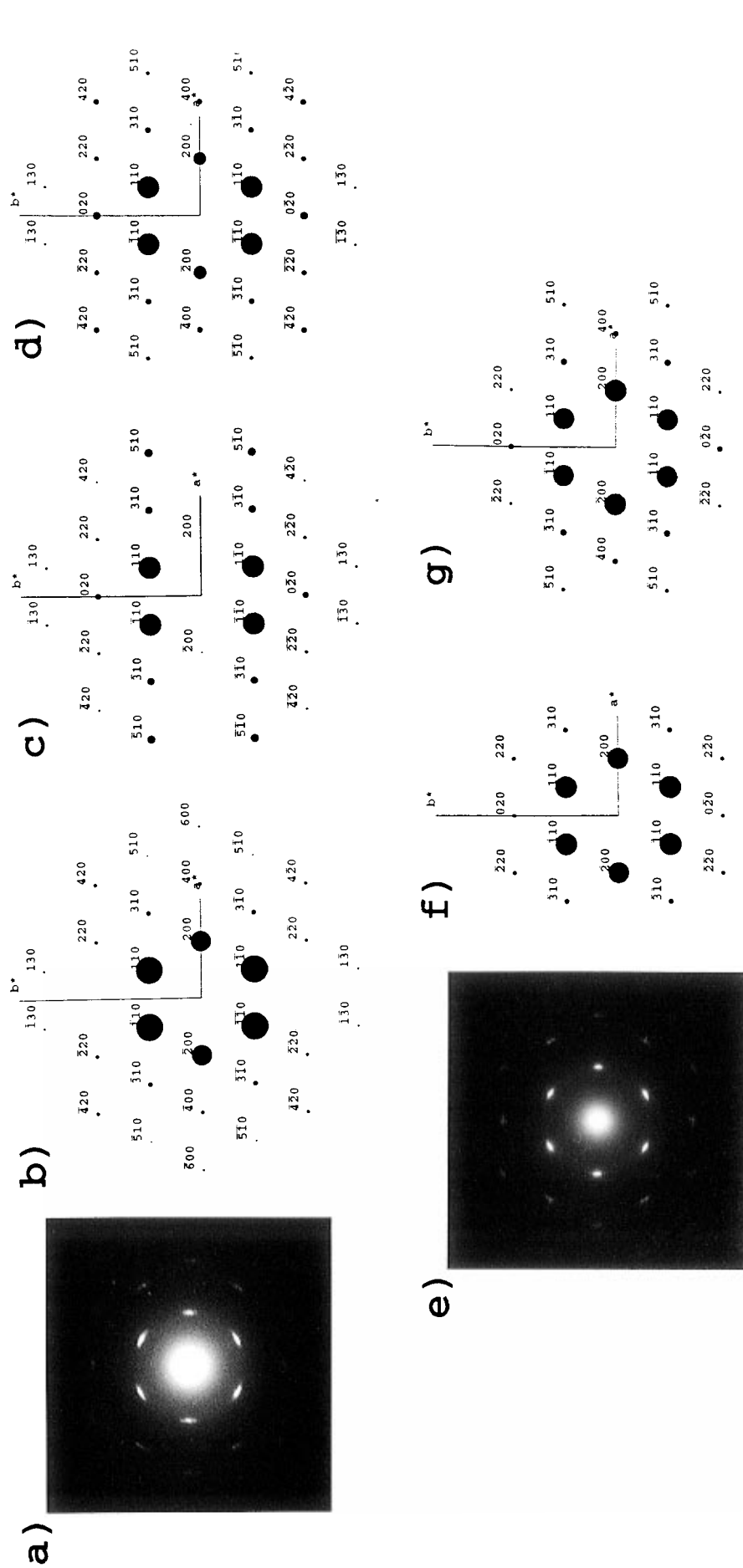
Results

Crystalline Structure of Model Compounds for Nylons *n*,3. A schematic representation of the model molecules pMPMp and pMBMp (1,4-bis(((propylamino)-malonyl)amino)butane) is shown in Figure 1b together with the definition of internal rotation angles. A summary of torsion angles and hydrogen-bond geometry of pMPMp, together with those previously reported for pMBMp,³ is given in Table 2. Molecular symmetry is characterized by a mirror plane through the center of the polymethylene segment and perpendicular to the chain axis. Thus, the torsion angles of the two halves of the molecules are equal but with opposite signs. Thus

Table 2. Selected Torsion Angles and Hydrogen-Bond Geometry for pMBMp³ and pMPMp

	pMBMp	pMPMp
Torsion Angles (deg)		
$C_A C_B C_C N_0$	180	-178
$C_B C_C N_0 C_{M1}$	-114	-112
$C_C N_0 C_{M1} C_{M2}$	180	-177
$N_0 C_{M1} C_{M2} C_{M3}$ (ψ_1)	114	114
$C_{M1} C_{M2} C_{M3} N_1$ (ψ_2)	111	111
$C_{M2} C_{M3} N_1 C_1$ (ω_1)	178	-178
$C_{M3} N_1 C_1 C_2$ (φ_1)	-105	-105
$N_1 C_1 C_2 C_3$ (ν_1)	178	180
$C_1 C_2 C_3 C_4$ (ν_2)	180	180
Hydrogen-Bond Geometry		
$d(H_0 \cdots O_1)$ (Å)	2.0	2.0
$d(N_0 \cdots O_1)$ (Å)	2.8	2.8
$\angle N_0 H_0 \cdots O_1$ (deg)	171	168
$d(H_1 \cdots O_2)$ (Å)	2.0	2.0
$d(N_1 \cdots O_2)$ (Å)	2.8	2.8
$\angle N_1 H_1 \cdots O_2$ (deg)	170	167

the pMPMp molecule has a defined orientation in the crystal, in spite of its chemical symmetry, since both halves have opposite conformations. It is worth noting the similar values of the torsional angles φ_i , ψ_i , and ν_i found in the model compounds independently of the number of methylenes (even or odd) in the diamine. Thus the model studies indicate $st_3\bar{s}$ and $st_4\bar{s}$ conforma-



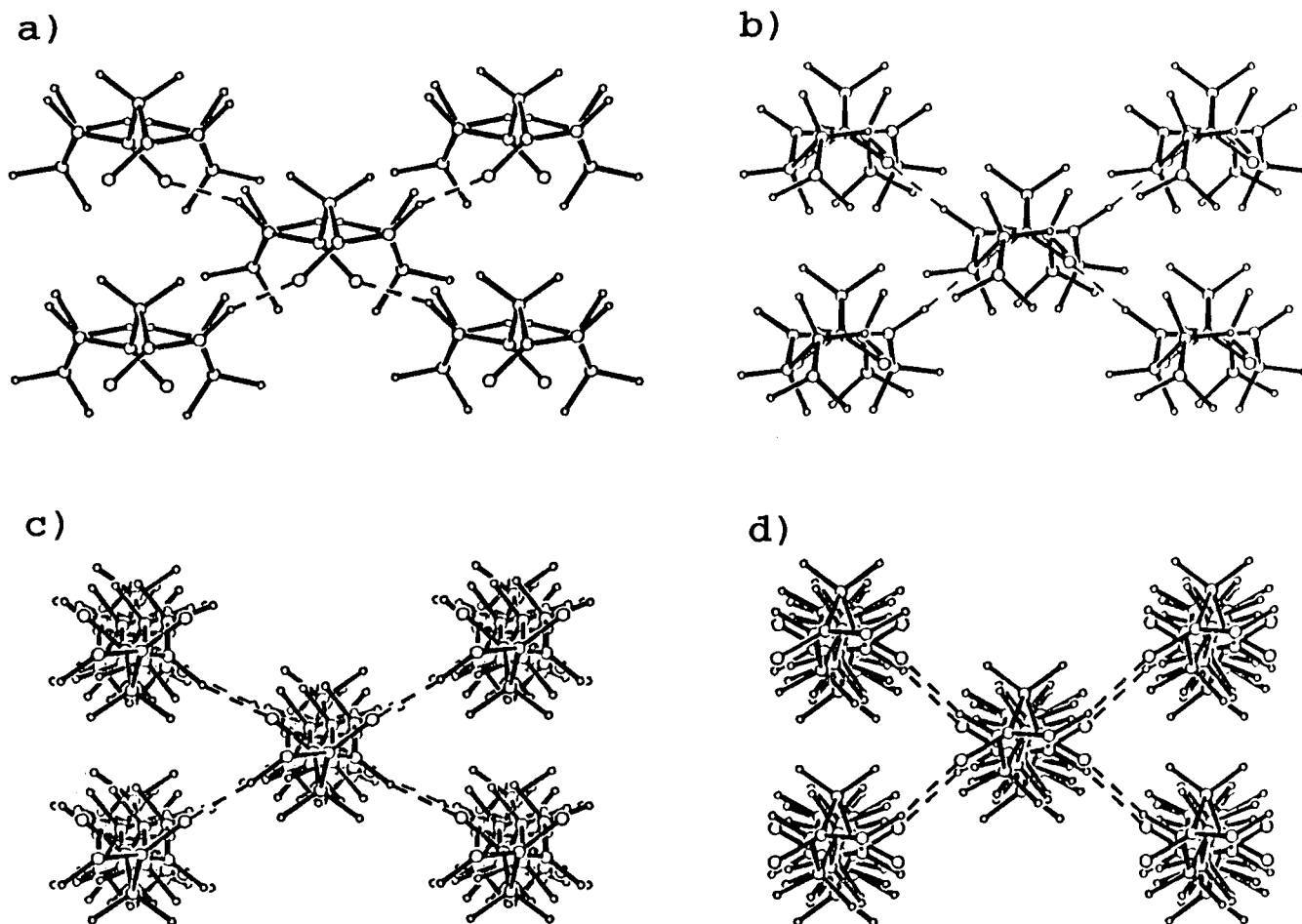


Figure 4. Equatorial projections of a central molecule and its four hydrogen-bonded neighbours for models II (a) and F (b) of nylon 5,3, and model I (c) and F (d) of nylon 6,3. The experimental results give support to the more symmetric models shown in b and d.

tion for the diamine units, which have also been suggested for linear polyamides in the γ form.^{5,10} On the other hand, the malonamide units have a characteristic conformation which induces a 120° rotation between amide groups and which is responsible for the unique hydrogen-bond system present in the solid state. A projection of the structures of pMBMp and pMPMp is shown in Figure 2 (a and b). It can be seen that each molecule is hydrogen-bonded with four neighboring molecules along two directions which form an angle of about 120° . Due to the mirror plane symmetry of the pMPMp molecules, the carbonyl groups of the two malonyl units point into the same direction and thus each molecule has a net dipolar moment. This is not the case for centrosymmetric compounds (i.e., pMBMp) which have an even number of methylenes in the diamine unit. pMPMp crystallizes in a $P12_1/m1$ space group, so the unit cell has two layers of molecules along the b crystal axis. Molecules in successive layers are rotated 180° , and thus, the crystal has no net dipolar moment. The surface of the layers is occupied by the terminal propyl groups, which have high temperature factors (the equivalent isotropic thermal parameter determined for the terminal carbon in pMPMp was 13.2 \AA^3). Thus, the interaction between neighboring layers is mainly due to weak van der Waals forces, which may be responsible for the mosaicity observed. The monoclinic unit cell indicates that molecules of a layer are not shifted along the b axis ($\alpha = \beta = 90^\circ$). On the contrary, molecules were shifted in the related com-

Table 3. Conformational Parameters and Hydrogen-Bond Geometry for Different Models of Nylons 5,3 and 6,3

	nylon 5,3			nylon 6,3	
	model I	model II	model F	model I	model F
space group	$C222_1$	$Cc2m$	$Cc2m$	$C12/c1$	$C12/c1$
torsion angles (deg)					
ψ_1	117	124	110	117	106
ψ_2	117	124	110	117	106
φ_1	-162	-99	-79	-103	-100
ν_1	107	180	179	180	-164
ν_2	178	180	154	180	172
ν_3	178	180	-154	180	180
ν_4	107	180	-179	180	-172
ν_5				180	164
φ_2	-162	99	79	103	100
ψ_1'	117	-124	-110	-117	-106
ψ_2'	117	-124	-110	-117	-106
φ_1'	-162	99	79	103	100
ν_1'	107	180	-179	180	164
ν_2'	178	180	-154	180	-172
ν_3'	178	180	154	180	180
ν_4'	107	180	179	180	172
ν_5'				180	-164
φ_2'	-162	-99	-79	-103	-100
ω_1	180	180	180	180	180
hydrogen-bond geometry					
$d(\text{H}\cdots\text{O})$ (Å)	1.93	1.69	1.72	1.74	1.86
$d(\text{N}\cdots\text{O})$ (Å)	2.88	2.63	2.73	2.73	2.85
$\angle\text{NHO}$ (deg)	156	151	171	171	167
R^a factor (%)	35	35	16	38	26

^a From electron diffraction data of single crystals.

pound pMBMp in order to improve the hydrogen-bond geometry (Figure 2c). In the same way, as will be discussed below, the corresponding nylons $n,3$ have

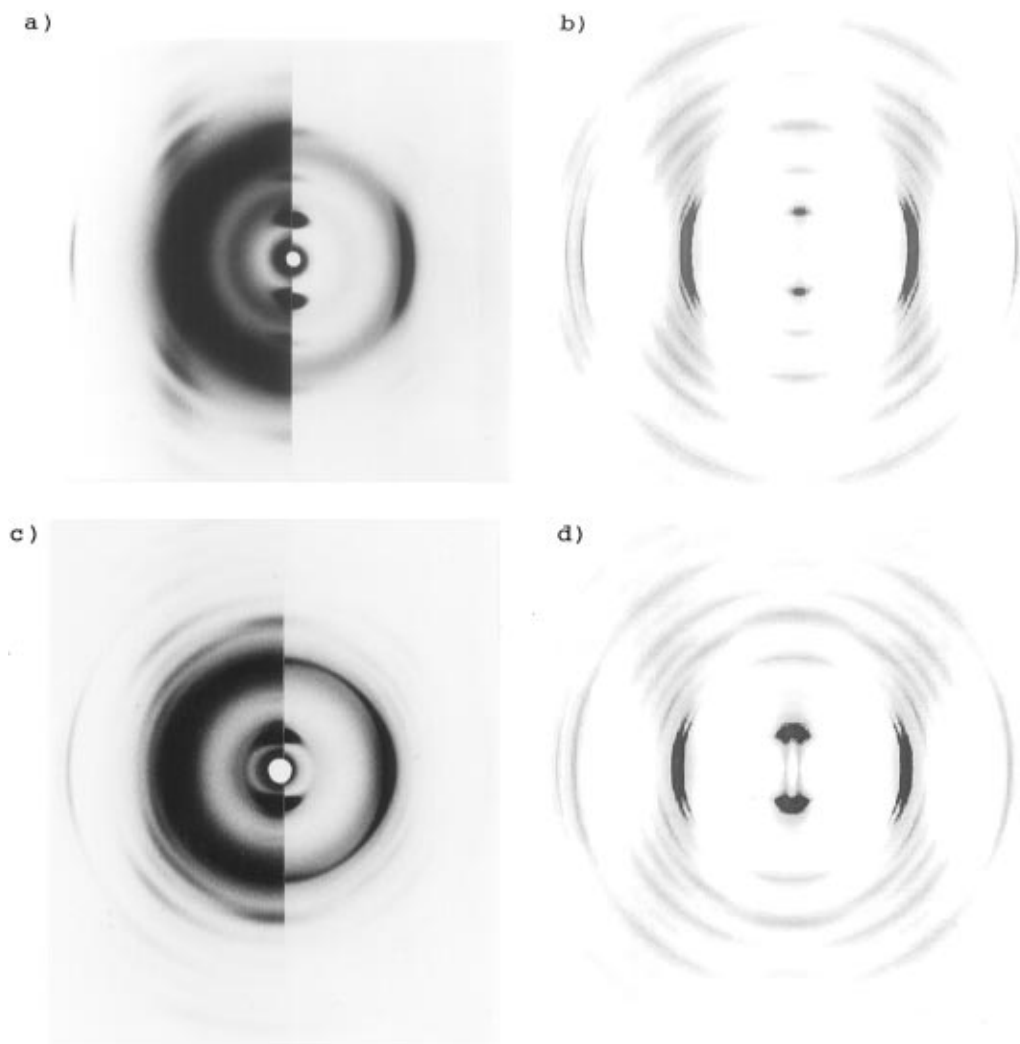


Figure 5. X-ray diffraction patterns of oriented films of nylons 5,3 (a) and 6,3 (c), and simulated patterns obtained with the CERIUUS program for models F of nylons 5,3 (b) and 6,3 (d).

different unit cells depending on the value of n (odd or even).

Structural Models for Nylon 5,3. X-ray and electron diffraction data¹ show that nylon 5,3 crystallizes in a centered orthorhombic unit cell with parameters $a = 8.47$ Å, $b = 4.62$ Å, c (chain axis) = 22.40 Å. It has also been conclusively demonstrated that molecules are organized in a network of hydrogen bonds with two spatial orientations. This particular hydrogen bond geometry can be explained by taking into account the conformational preferences ($\psi_1 \approx \psi_2 \approx 115^\circ$) found for the malonyl residues in the model compounds.^{2,3} In fact, the different models studied in this paper (Table 3) are based on this particular conformation. The experimental value of the c parameter indicates that the chain repeat has two monomer units. Thus, in the refining process of nylon 5,3, we have considered the different symmetry elements which relate these two monomer units and also the different conformations available for the diamine moiety. In this sense the systematic absences detected in the diffraction patterns are in agreement with a 2-fold screw axis (model I) or a glide plane (models II and F). In the first case, nylon 5,3 will have no dipole moment as the corresponding crystals of the pMPMp model compound, whereas in the second case, the symmetry of the molecular chain is closer to that observed for pMPMp.

Model I. A 2-fold screw axis symmetry for the molecular chains of nylon 5,3 is feasible when the pentamethylene moiety causes a ca. 120° rotation between the amide groups in order to compensate for the rotation imposed by the malonamide units. The adirectional configuration of the molecular chains is preserved with additional symmetry elements as a binary axis perpendicular to the chain direction through the malonyl residue (derived from their particular conformation $\psi_1 = \psi_2$) and a binary axis or a mirror plane perpendicular also to the chain direction through the middle of the pentamethylene segment. Since a mirror plane will not induce any rotation of the amide groups, we assume an $s(2/1)2$ symmetry for the molecular chain. With these assumptions, the model was refined with the following torsion angles constraints: $\psi_1 = \psi_2$, $\varphi_1 = \varphi_2$, $\nu_1 = \nu_4$, and $\nu_2 = \nu_3$. Although the model appears stereochemically suitable and all hydrogen bonds are formed with length and angle values within the standard ranges (Table 3), the model is not consistent with the observed electron diffraction data. The disagreement R factor ($\sum |F_o - F_c| / \sum F_o$) for the electron diffraction data was optimized with a temperature factor of 0 Å². Such an unrealistic value is a common feature in the structural refinement of electron diffraction data when crystal bending effects or dynamical scattering are not taken into account.¹¹ However, the discrepancy index becomes 35%, a value too high even

Table 4. Observed (F_o) and Calculated (F_c) Electron Diffraction Structure Factors for Models of Nylons 5,3 and 6,3

hkl	m^a	nylon 5,3				nylon 6,3			
		F_o^b	model I ($R_t = 35\%$)	model II ($R_t = 35\%$)	model F ($R_t = 16\%$)	F_o^b	model I ($R_t = 38\%$)	model F ($R_t = 26\%$)	
200	2	8.0	7.6	0.8	6.1	10.0	9.6	10.0	
110	4	10.0	10.0	10.0	10.0	9.8	10.0	9.7	
310	4	4.0	1.8	3.3	2.7	4.8	2.3	2.9	
020	2	3.6	0.0	2.8	3.6	4.0	1.8	2.7	
400	2	4.0	1.4	0.1	2.6	3.7	0.4	2.7	
220	4	3.3	1.4	1.6	2.3	3.5	1.9	1.4	
510	4	2.0	0.6	3.7	1.9	2.6	0.0	1.9	
420	4	2.4	1.4	1.0	2.7	2.4	0.4	0.5	
130	4	2.0	0.9	1.3	1.2	1.0	0.3	0.4	

^a Multiplicity. ^b All equivalent spots have a similar intensity.

for electron diffraction analysis. Furthermore, only the six inner spots of the $hk0$ electron diffraction pattern have an intensity comparable with those calculated (Figure 3 and Table 4). Thus, the computed structure factors of the remaining reflections were in general lower than the observed ones. In particular, the calculated structure factor for the 020 reflection does not coincide at all with the observed value.

Model II. In this case a conformation with $\varphi_1 \approx -\varphi_2 \approx -100^\circ$ and $\nu_i = 180^\circ$ was determined for the diamine moiety (Table 3). This conformation is similar to the one detected for the model compound pMPMp and corresponds to the conformational arrangement $st_4\bar{s}$, characteristic for a γ conformation. Molecular chains respectively have (in addition to the c glide plane) a binary axis and a mirror plane perpendicular to the chain direction through isolated methylene groups and through the middle of the $-(CH_2)_5-$ methylene segment. This molecular symmetry (tcm) has the consequence that equivalent torsional angles in consecutive repeat units are equal but with opposite sign. Furthermore, the expected adirectional configuration of the polymer chains is well-preserved. A space group $Cc2m$ is compatible with molecular symmetry and also with the mm symmetry of the $hk0$ electron diffraction pattern. All hydrogen bonds are formed with length and angle values within the standard ranges (Table 3), and no significant contacts were found. Although this model appears plausible on stereochemical grounds, it also turns out to be inadequate when the observed and calculated diffraction data are compared (Figure 3 and Table 4). In particular, an unacceptable structure factor is computed for the 200 reflection which does not compare at all with the observed value.

Model F. The R factor was considerably improved when we allowed that the ν_i torsional angles deviate slightly from the *trans* conformation. In fact, previous results on some oligomer models^{12,13} demonstrate that an extended conformation for the polymethylene segments is not always preferred. The symmetry of model II is maintained with the constraints: $\nu_1 = -\nu_4$ and $\nu_2 = -\nu_3$. Figure 4a,b compares the equatorial projection of the unit cell of models II and III. It can be seen that the projection of a molecular chain becomes more cylindrical when the ν_i torsional angles are different from 180° . Thus, the distribution of intensities of the $hk0$ electron diffraction pattern will be quasi-hexagonal, as can be seen by the enhancement of the 200 reflection (Figure 3 and Table 4).

Figure 5a,c compares the experimental and simulated X-ray diffraction patterns of oriented films of nylon 5,3, whereas computed intensities and experimental data are summarized in Table 5. A satisfactory agreement was found for all equatorial, meridional, and off-me-

Table 5. Experimental and simulated X-ray diffraction data for models III and II of nylons 5,3 and 6,3, respectively

nylon 5,3			nylon 6,3		
index ^a	I_{obs}^b	I_{cal}	index ^c	I_{obs}^b	I_{cal}^d
Equatorial					
200; 110	vs	231	200; 110	vs	288
310	m	7.0	310	s	3.6
020	w	6.4	020	m	4.6
400	w	4.0	400	w	1.6
220	w	2.0	220	vw	1.0
Meridional					
002	vs	16	002	vs	28
004	m	3.8	004	w	0.2
006	s	2.5	006	m	6.0
008	w	6.4	008	s	18
0010	vw	0.6	0010	w	9.2
Off-Meridional					
202; 112	m	10	204; 113; 112	m	1.2; 1.2; 0.4
203; 113	m	7.0	205; 114; 113	m	0.0; 1.0; 8.6
204; 114	m	16	206; 115; 114	s	9.4; 0.4; 3.2
205; 115	s	22	207; 116; 115	w	0.0; 0.0; 7.4
206; 116	s	21	208; 117; 116	m/s	7.6; 0.0; 10.8
207; 117	w	3.8	209; 118; 117	w	0.0; 1.4; 2.2
208; 118	m	25	20.10; 119; 118	m	1.8; 2.8; 15
209; 119	w	9.6	20.11; 11.10; 119	w	1.2; 3.2; 3.8
20.10; 11.10	w	8.2	20.12; 11.11; 11.10	m	0.0; 11; 1.8

^a On the basis of an orthorhombic unit cell: $a = 8.47$ Å, $b = 4.62$ Å, and $c = 22.40$ Å. ^b Abbreviations: vs, very strong; s, strong; m, medium; w, weak; vw, very weak. ^c On the basis of a monoclinic unit cell: $a = 8.60$ Å, $b = 4.62$ Å, $c = 25.70$ Å, $\alpha = 90^\circ$, $\beta = 100.4^\circ$, and $\gamma = 90^\circ$. ^d The intensity of the different reflections which contribute to the same off-meridional spot has been indicated. Only the 201 reflections have been omitted to their low intensity.

ridional reflections. It is worth noting that the intensity calculations show 008 as the more intense meridional reflection. This is not clear in the film and the simulated diffraction patterns due to the curvature of the Ewald sphere. However, this reflection appears as the most intense when the film is tilted with respect to the X-ray beam.¹

No significant contacts were found in this model. Moreover the hydrogen bond geometry was improved since the $\angle NHO$ angles become more linear. In conclusion, this arrangement appears to us as the most adequate for the nylon 5,3 chain. Molecular drawings of a linear projection of three hydrogen-bonded chains are shown in Figure 6a, whereas the fractional coordinates of the asymmetric unit are given in Table 6.

Structural Models for Nylon 6,3. X-ray diffraction patterns of oriented films of nylon 6,3¹ indicate a monoclinic unit cell and a value of the c parameter (chain axis) equal to twice the length of one monomeric unit. From X-ray and electron diffraction data, a unit cell of parameters $a = 8.60$ Å, $b = 4.62$ Å, $c = 25.70$ Å,

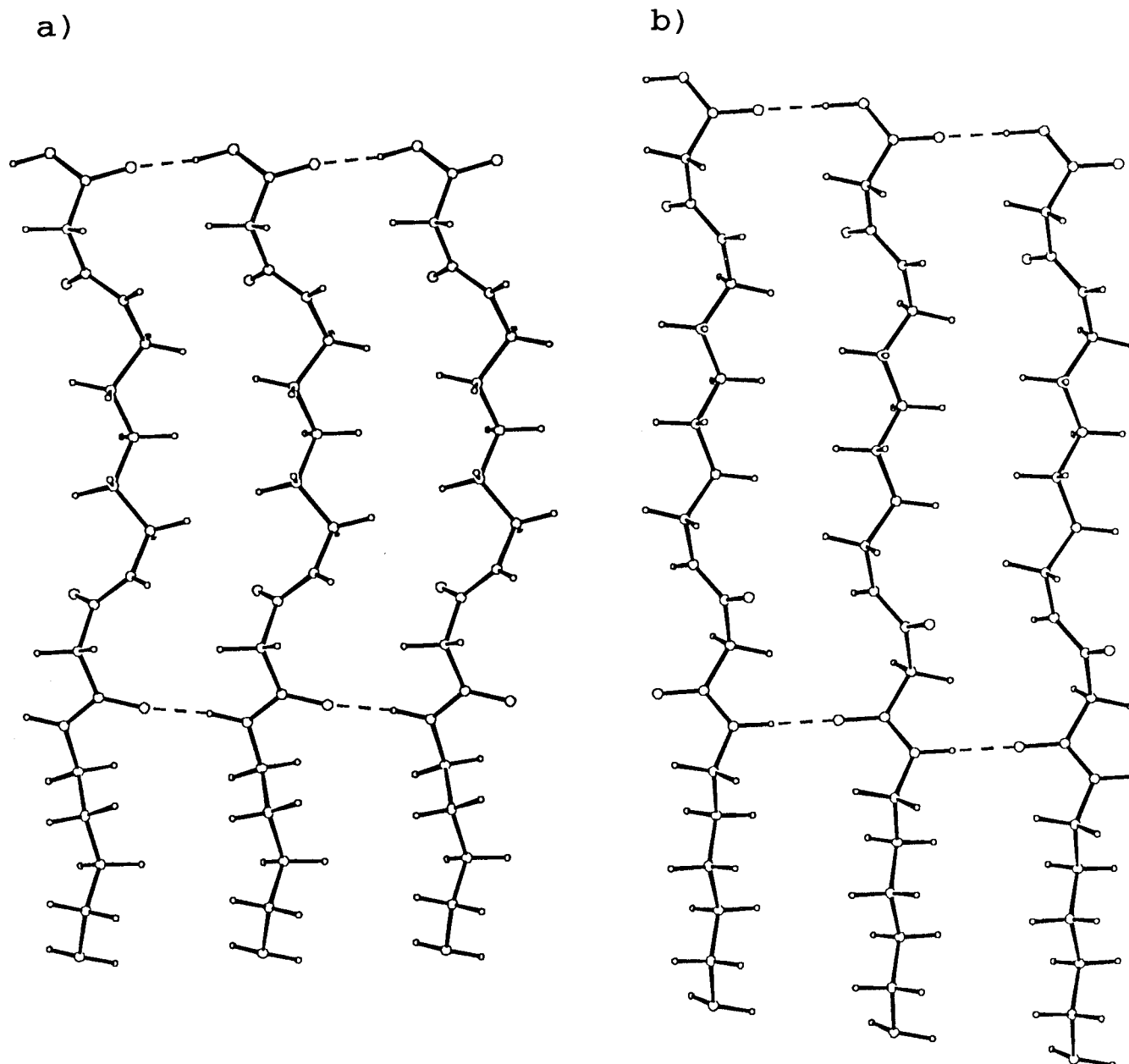


Figure 6. Lateral view perpendicular to one hydrogen-bond direction of three neighboring chains of the optimal models of nylon 5,3 (a) and 6,3 (b). Note the different molecular symmetry and the characteristic shift along the chain axis for nylon 6,3.

Table 6. Fractional Coordinates for the Optimized Models of Nylons 5,3 and 6,3 (Molecular Axis at $x = 0, y = 0$)^a

atom	nylon 5,3			nylon 6,3		
	<i>x</i>	<i>y</i>	<i>z</i>	<i>x</i>	<i>y</i>	<i>z</i>
C _{M2}	0.00	0.22	0.00	0.00	0.25	0.25
C _{M1}	0.00	0.03	0.06	-0.04	0.06	0.21
O ₂	0.12	-0.11	0.07	-0.17	-0.07	0.20
N ₁	-0.23	0.15	0.08	0.07	0.04	0.17
H ₁	-0.15	-0.13	0.14	0.17	0.15	0.18
C ₁	-0.06	0.02	0.19	0.05	-0.13	0.13
C ₂	-0.08	-0.16	0.25	0.00	0.07	0.08
C ₃				0.01	0.09	0.03

^a Units cells are given in the text and in Table 5.

$\alpha = 90^\circ$, $\beta = 100.4^\circ$, and $\gamma = 90^\circ$ was conclusively demonstrated. Moreover, the experimental evidences indicate that nylon 6,3 has two hydrogen-bond directions in the crystalline state. As in nylon 5,3, the models that compare best with the experimental data are based on a *c* glide plane as symmetry element which

relates the two monomeric units and also on the particular conformation of the malonamide unit: $\psi_1 = \psi_2 \approx 115^\circ$. Moreover, an inversion center in the middle of the polymethylene segment ensures the adirectional configuration when the diamine moiety has an even number of methylene units. A conventional conformation like an extended or a γ -form is assumed for the diamine unit. In fact, the experimental data obtained for the pMBMp model compound are in agreement with a γ conformation. Thus the expected molecular symmetry is *tic*, with the binary axis (derived from the glide plane and the inversion center) perpendicular to the chain direction and to the *c* glide plane through the isolated methylene group of the malonamide unit. The torsional angle constraints $\psi_1 = \psi_2$, $\varphi_1 = -\varphi_2$, $\nu_1 = -\nu_5$, and $\nu_2 = -\nu_4$ were imposed in the refinement process taking into account this symmetry. The resulting space group was *C12/c1* when we kept the molecular symmetry and considered the packing which gives the optimum hydrogen-bond geometry. Thus, the binary

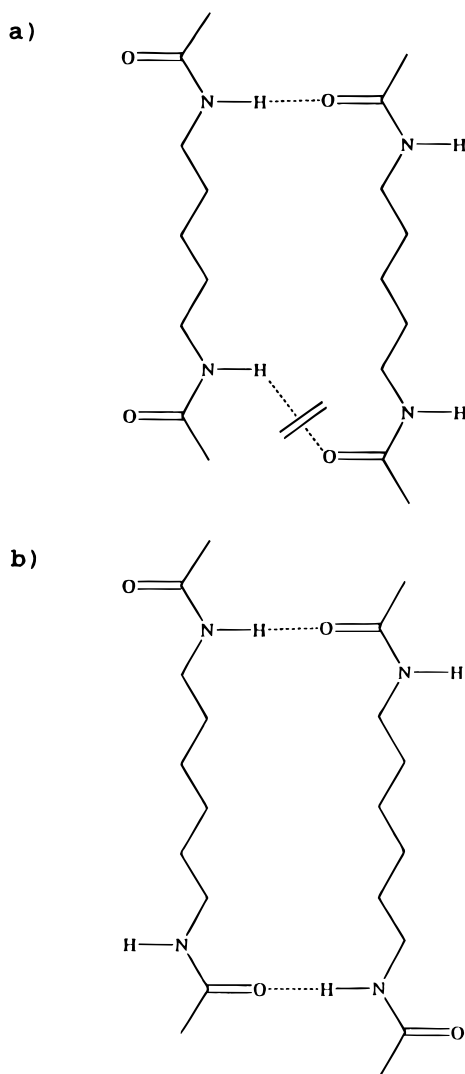


Figure 7. Schematic representation showing the different results obtained when molecular chains are shifted along the chain axis direction for nylons with either an odd (a) or even (b) number of methylenes in the diamine unit. Note that only 50% of hydrogen bonds with optimum geometry are established when the number is odd. In that case, the plane of the amide groups is inclined with respect to the main chain direction and an orthorhombic cell appears, as shown in Figure 6.

axis has to be parallel to the short side of the unit cell, since the conformation of the malonamide unit imposes a 120° rotation between its two amide groups. Note also that the monoclinic angle is β according to the experimental evidence.¹ Furthermore, the *mm* symmetry of the *hk0* electron diffraction pattern is also justified with the selected space group. The unit cell differences between nylons 5,3 and 6,3 can be well-explained by considering both the odd or even number of methylenes in the diamine moiety and the optimum hydrogen-bond geometry. Thus, for an even number of methylenes, the two amide groups point into opposite directions and hydrogen bonds become more linear when neighboring chains are shifted in the chain axis direction. This is not feasible when the number of methylene units is odd, and in this case an orthorhombic packing is preferred instead of a monoclinic one (Figure 7).

As in nylon 5,3, we have considered that the methylene torsional angles of the diamine moiety were either fixed at 180° (model I) or were allowed to deviate from the *trans* conformation (model F). Table 3 summarizes the main characteristics of the two models. Although

they appear stereochemically suitable and give a reasonable hydrogen-bond geometry, the electron diffraction refinement clearly points to model F (Table 4 and Figure 3). Thus in Model I, the more intense reflections (200 and 100 or $\bar{1}10$) appear with inverted intensities. Also, the 400 reflection is calculated to be very weak, in disagreement with the experimental observations. On the contrary, the simulated electron diffraction pattern of model F compares well with the experimental data. In fact, the diffraction pattern becomes quasi-hexagonal as a result of the more cylindrical projection of the molecular chains when the ν_i angles are slightly different from 180° . Note that the same conclusion was reached in the analysis of the nylon 5,3 structure.

The X-ray diffraction pattern of oriented films was also adequately simulated with the atomic coordinates of model F (Figure 5d). Furthermore, an acceptable agreement between observed and calculated intensities was attained (Table 5). Note the resemblance between the experimental and simulated meridional spots, both patterns with a weak 004 reflection. Indexing of the off-meridional reflections was difficult since the disorientation angle results in the superposition of spots from several layer lines. Since all calculated 201 reflections were weak, we assume that the experimental spots result from the superposition of the appropriate 111, $\bar{1}11+1$ and $201+2$ reflections. In the case of the 206 and 208 spots, they were clearly apparent in the diffraction pattern, in agreement with their computed intensities. Only the intensity of the 3.87 \AA reflection deviates from the calculated values. However, we have to consider that the observed intensity of this spot is enhanced by the contribution of the arched equatorial reflections and the amorphous halo.

Figure 6b shows a lateral view perpendicular to one hydrogen bond direction of three neighboring chains. Note that the molecular chains are shifted in order to establish hydrogen bonds and the polymethylene segments deviate slightly from an *all-trans* conformation. Fractional coordinates of the asymmetric unit of nylon 63 are given in Table 6.

Discussion

The model studies presented in this paper demonstrate that it is indeed possible to build an adequate model consistent with the experimental diffraction data. The models for both types of nylons *n*,3 (*n* = even or odd) show a three-dimensional network of hydrogen bonds with two preferred orientations which form an approximate angle of 120° , in agreement with the experimental results available.¹ Thus, the *n*,3 polyamides have a unique conformation within the nylon family of compounds.

A somewhat surprising feature of the final model F is the fact the polymethylene segments are not in an *all-trans* conformation but deviate somewhat from 180° , as shown in Table 3. The final angles determined should not be taken to indicate a rigid conformation. Instead, it is likely that there is some librational movement in the polymethylene segment so that each ν_i angle may vary around the extended chain value of 180° by a certain amount. The maximum variation suggested by the F model is 26° (ν_2 and ν_3 values for the nylon 5,3 model). This situation might be analogous to the mobility of the methylene segments above the Brill transition.¹⁴ Also, a similar deviation from the *all-trans* conformation has been found in some related model compounds.¹³

Acknowledgment. We are thankful to Drs. V. Tereshko and X. Solans for their help in the collection and processing of the X-ray data presented here. E.N. and J.E.A. acknowledge financial support from the Department d'Ensenyament de la Generalitat de Catalunya (DGU). This work has been supported in part by a DGICYT grant PB93-1067 and a DGU grant GRQ93-3030.

References and Notes

- (1) Aceituno, J. E.; Tereshko, V.; Lotz, B.; Subirana, J. A. *Macromolecules* **1996**, *29*, 1886.
- (2) Tereshko, V.; Navarro, E.; Puiggali, J.; Subirana, J. A. *Macromolecules* **1993**, *26*, 7024.
- (3) Navarro, E.; Puiggali, J.; Subirana, J. A. *Macromol. Chem. Phys.* **1995**, *196*, 2361.
- (4) Holmes, D. R.; Bunn, C. W.; Smith, D. J. *J. Polym. Sci.* **1955**, *17*, 159.
- (5) Kinoshita, Y. *Makromol. Chem.* **1959**, *33*, 21.
- (6) Strube, R. E. *Org. Synth.* **1957**, *37*, 34.
- (7) Sheldrick, G. M. *SHELXS-86 Program for Crystal Structure Determination*, University of Oxford: Oxford, England, 1986.
- (8) Sheldrick, G. M. *SHELXS-93 Program for refinement of crystal structures*, Institut fuer Anorganische Chemie: Goettingen, Germany, 1993.
- (9) Campbell-Smith, P.; Arnott, S. *Acta Crystallogr., Sect A* **1978**, *34*, 3.
- (10) Arimoto, H.; Ishibashi, M.; Hirai, M.; Chatani, Y. *J. Polym. Sci., Part A* **1965**, *3*, 317.
- (11) Moss, B.; Dorset, D. L. *J. Polym. Sci. Polym. Phys.* **1982**, *20*, 1789.
- (12) Navarro, E.; Alemán, C.; Puiggali, J. *J. Am. Chem. Soc.* **1995**, *117*, 7307.
- (13) Navarro, E.; Tereshko, V.; Subirana, J. A.; Puiggali, J. *Biopolymers*, **1995**, *36*, 711.
- (14) Wendoloski, J. J.; Gardner, K. H.; Hirschinger, J.; Miura, H.; English, A. B. *Science* **1990**, *247*, 431.

MA960069K